International Journal for Computational Civil and Structural Engineering, 20(4) 186–196(2024)

DOI:10.22337/2587-9618-2024-20-4-186-196

TO THE MATHEMATICAL ESTIMATION OF THE STRAIN SENSORS ERROR

Nelly N. Rogacheva, Vladimir N. Sidorov, Yulia G. Zheglova

National Research Moscow State University of Civil Engineering, Moscow, RUSSIA

Abstract: The work is devoted to the mathematical analysis of the error of the theory of strain sensors. In the theory of deformation sensors, it is assumed that the sensor, due to its geometric and mechanical characteristics, does not make changes (or makes minor changes) to the stress-strain state (SSS) of the tested structure. To numerically estimate the sensor error, an exact solution of the dynamic contact problem of the sensor and the elastic half-space is obtained. For the analytical solution of the problem, the method used by Lamb to determine the dynamic stress-strain state of an elastic half-space under the action of concentrated forces applied to its surface is generalized. A numerical solution of this problem has been performed for sensors and elastic half-space made of various materials. Practical recommendations are formulated. A numerical solution of this problem has been performed

Keywords: stress-strain state, strain sensor, contact problem, Lamb problem, error estimation

К МАТЕМАТИЧЕСКОЙ ОЦЕНКЕ ПОГРЕШНОСТИ ДАТЧИКОВ ДЕФОРМАЦИЙ

Н.Н. Рогачева, В.Н. Сидоров, Ю.Г. Жеглова

Национальный исследовательский Московский государственный строительный университет, г. Москва, РОССИЯ

Аннотация: Работа посвящена математическому анализу погрешности теории датчиков деформаций. В теории датчиков деформаций предполагается, что датчик в силу своих геометрических и механических характеристик не вносит изменений (или вносит незначительные изменения) в напряженно-деформированное состояние (НДС) испытуемой конструкции. Для численной оценки погрешности датчика получено точное решение динамической контактной задачи датчика и упругого полупространства. Для аналитического решения этой задачи обобщен метод, который использовал Лэмб для определения динамического напряженно-деформированного состояния упругого полупространства под действием сосредоточенных сил, приложенных к его поверхности. Выполнено численное решение этой задачи для датчиков и упругого полупространства из различных материалов. Сформулированы практические рекомендации.

Ключевые слова: напряженно-деформированное состояние, датчик деформации, контактная задача, задача Лэмба, оценка погрешности

INTRODUCTION

The history of the emergence and use of strain sensors begins in the middle of the 19th century with the invention by Professor Thomson (known as Lord Kelvin) of the first sensor for measuring elongation (compression) strains [1] on the surface of the structure under study. To ensure reliable operation of the structure, as a rule, the analytical or numerical calculation of the structure should be supplemented and verified with experimental studies of its stress-strain state (SSS). If the results of the calculation and experiments differ slightly, then the calculation is correct. In particularly difficult cases, when it is impossible to obtain a sufficiently accurate solution to the problem, the role of the experiment is irreplaceable. The main role in BIM technology in construction, as well as in monitoring the responsible for unique

buildings and structures, is played by long-term experimental observation of the state of the structure. This is why it is very important to estimate the error of experiments.

The measurement error of strain sensors analysis is a complex problem, since it is necessary to estimate both the error of the theory of sensors and the error of experimental measurements.

We will consider the error of the theory of strain sensors using the example of the most common sensor of Lord Kelvin. The obtained conclusions are also suitable for new types of piezoelectric sensors [2-3].

Lord Kelvin was the first to notice that the deformation of a conductor is accompanied by a change in its electrical resistance. By measuring the change in resistance, its deformation can be detected. The first strain sensor, Lord Kelvin's strain sensor, is based on this fact. The change in resistance is extremely small, but it can be amplified and measured using additional equipment.

The theory of the piezoelectric sensor was constructed and confirmed by experiments in [2]. Thin-walled elements made of pre-polarized ceramics with a strong piezoelectric effect were used as the sensor. The front surfaces of the piezoelectric element were covered with electrodes. The piezoelectric sensor was glued to the surface of the deformed body and deformed together with it. The operation of the sensor is based on the use of the direct piezoelectric effect. The direct piezoelectric effect is as follows: when the piezoelectric element is mechanically loaded, an electric charge appears on its electrodes. For a material with a strong piezoelectric effect, a significant part of the mechanical energy of the deformed piezoelectric element is converted into electrical energy. Tangential deformations were calculated based on the measured difference in electrical potentials on the electrodes.

The error of the sensor theory is the error of the contact problem of the sensor and the structure under study. It should be noted that insufficient attention is paid to the estimation of the error of the main hypotheses of the theory of deformation sensors in research. As a rule, research is devoted to sensor calibration, experimental measurement errors, errors in the description of material properties, etc. [4-11]. In the paper, we will evaluate the validity of the sensor theory.

Each sensor measures one integral characteristic. For example, the integral characteristic of the Kelvin sensor is the change in resistance. The change in the cross-sectional area of the conductor is used to calculate the change in the resistance of the conductor and its deformation.

For a piezoelectric sensor, the integral characteristic is the difference in electric potential on its electrodes. Based on this measured value of the difference in electric potential, the corresponding component of the strain tensor at the point of the test object is calculated.

APPROXIMATE DETERMINATION OF THE SSS OF A STRAIN SENSOR

The contact problem of a sensor and a body under study is a complex mathematical problem. For simplicity of research, we will assume that we measure the elongation or compression strain at a point on the surface of an elastic half-space using a sensor. Figure 1 shows the sensor and the elastic half-space related to the Cartesian coordinate system. It is assumed that the sensor has a length $2l$, a thickness τ and is infinite in the direction x_2. We will investigate the deformation of e_1 in the direction x_1. To simplify the problem, we will assume that our solution does not depend on x_2.

We will assume that the elastic half-space performs harmonic oscillations under the action of a load changing according to the law $e^{-i\omega t}$, where i is an imaginary unit, t is time, ω is the circular frequency of oscillations. Since the oscillations are harmonic, all equations can be written relative to the amplitude values of the

sought quantities. Note that the solution to the contact problem does not depend on the coordinate x_2.

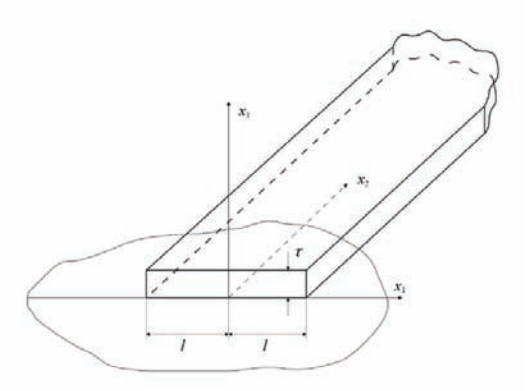

Figure 1. Schematic representation of the sensor on the surface of the elastic half-space

To solve our problem, we will use the iteration method. Describing the zero approximation of the solution to the problem, we assume that the sensor satisfies all the conditions of its applicability for measuring deformations:
-in the contact area of the sensor and the structure under study, the conditions of ideal contact are met;
-on the part of the body surface where the sensor is located, there is no surface load;
-the sensor is made of a material that slightly changes the stress-strain state of the body being studied in the area of its contact with the sensor;
-the characteristic length of the deformation pattern in the elastic half-space is greater than the width of the active element (this means that the variability of the sensor's SSS along the coordinate x_1 is small), which allows us to assume that the elongation (compression) deformation along the coordinate x_1 does not change.
In all sensor theories, it is assumed that the sensor does not introduce disturbance into the SSS of the test object, therefore, as a zero approximation of the iterative process, it is natural to assume that within the sensor, the elongation (compression) deformation in the direction of the axis does not depend on the variable x_1.
As a zero approximation of the contact problem, we assume that the longitudinal deformation of the half-space and the sensor are equal and are constant in the contact region. In this case, the contact condition for stresses is not satisfied. Then, at the next step of the iteration process, we will fulfill the contact condition for stress - we will remove the discrepancy that appeared at the previous step.
The equations describing the zero approximation of the sensor's SSS relative to the amplitude values have the following form (below are written only those equations that will be used for the zero approximation of solving the formulated contact problem):
Equation of motion

$$\frac{\partial \sigma_{11}}{\partial x_1} + \frac{\partial \sigma_{13}}{\partial x_3} + \rho \omega^2 u_1 = 0 \qquad (1)$$

Hooke's Law

$$\sigma_{11} = E e_1 \qquad (2)$$

Geometric equation relating deformation to displacement

$$e_1 = \frac{\partial u_1}{\partial x_1} \qquad (3)$$

In equations (1)-(3) σ_{11}, σ_{13} are stresses, e_1 are the component of the strain tensor in the direction x_1, and u_1 is the component of the displacement vector in the direction x_1.
Let us transform these equations.
Since, according to the assumptions made, the strain component e_1 does not depend on the variable x_1, then

$$e_1 = const \qquad (4)$$

By virtue of relation (2) the stress component also does not depend on the variable x_1.

$$\sigma_{11} = const \tag{5}$$

Taking into account (5), the equation of motion (1) becomes simpler and can be written as

$$\frac{d\sigma_{13}}{dx_3} + \rho\omega^2 x_1 e_1 = 0 \tag{6}$$

We integrate equation (4) and find that the displacement is an odd function x_1 and changes along the coordinate x_1 according to a linear law

$$u_1 = x_1 e_1 \tag{7}$$

From the accepted assumption of the absence of surface load on the outer surface of the sensor it follows

$$\sigma_{13}\big|_{x_3=\tau} = 0 \tag{8}$$

Integrating the equation of motion (6) with respect to the variable x_3 and satisfying condition (8), we obtain

$$\sigma_{13}\big|_{x_3=0} = x_1 \tau\rho\omega^2 e_1 \tag{9}$$

For further use, the stress σ_{13} should be continued as a periodic function of x_1 over the interval $[-L,+L]$, $L \geq 2l$ as follows:

$$\sigma_{13}(x_1) = \tau\rho\omega^2 e_1 \begin{cases} 2l - x_1 & l \leq x_1 \leq 2l \\ x_1 & -l \leq x_1 \leq l \\ -(2l + x_1) & -2l \leq x_1 \leq -l \end{cases}$$

$$\sigma_{13}(x_1) = \frac{4l\tau\rho\omega^2 e_1}{\pi^2} \sum_{n=0}^{N} (-1)^n \frac{1}{(2n+1)^2} \sin\frac{(2n+1)}{2l} x_1 \tag{10}$$

The function $\sigma_{13}(x_1)$ is chosen so that the function $F(x_1)$ is continuous in the interval $[-L,+L]$. In addition, the integral $\int_{-L}^{+L} F(x_1)dx$ must be equal to zero. Note that the function can be continued $[-L,+L]$ in any way that ensures rapid convergence of the solution.

The conditions of ideal contact of two deformable bodies are that at all points of the contact area of the bodies the displacements and stresses of both bodies are equal. In this particular case, instead of equality of displacements, equality of deformations can be used.

In the zero approximation of the iteration method, it was assumed that the deformations of the sensor and the half-space are equal. At the same time, on the contact surface, as shown by formula (9), the condition of ideal contact for stress σ_{13} is not satisfied. We will remove this discrepancy under contact conditions at the first step of the iteration process. To do this, we will calculate the elastic half-space loaded with surface load (9) in the region $-l \leq x_1 \leq l$. After performing the first step of the iteration process, a discrepancy in the equality of deformations in the contact region will appear. It is this value - the value of the maximum deformation of the half-space surface that serves in the contact region, serves as an estimate of the sensor error.

PROBLEM FOR AN ELASTIC HALF-SPACE

The complete system of equations describing an elastic half-space SSS $(x_3 \leq 0)$ includes equilibrium equations, geometric ratios relating deformations to displacements, and equations of state (Hooke's law).

Since analogous to the Lamb problem is considered, the equations are taken in the traditional form in terms of displacements. To solve the problem, the Lamb method is used, described in papers [12, 13] for the case of

concentrated forces applied at a point on the surface of an elastic body. In this paper, the Lamb method is generalized to the case of a distributed surface load. This generalized Lamb method was previously used in [14] to solve the dynamic contact problem of an actuator and an elastic half-space.

Following Lamb, the equilibrium equations are written as

$$\begin{aligned}(\lambda+\mu)\frac{\partial\theta}{\partial x_1}+\mu\nabla^2 u_1+\rho\omega^2 u_1=0\\(\lambda+\mu)\frac{\partial\theta}{\partial x_3}+\mu\nabla^2 u_3+\rho\omega^2 u_3=0\end{aligned} \tag{11}$$

where ∇^2 is the Laplace operator, θ is the volumetric deformation, λ and μ are the Lame coefficients:

$$\nabla^2=\frac{\partial^2}{\partial x_1^2}+\frac{\partial^2}{\partial x_3^2},\qquad \theta=\frac{\partial u_1}{\partial x_1}+\frac{\partial u_3}{\partial x_3} \tag{12}$$

$$\lambda=\frac{\nu E}{(1+\nu)(1-2\nu)},\quad \mu=\frac{E}{2(1+\nu)} \tag{13}$$

Stress-strain formulas with Lame coefficients are written as

$$\begin{aligned}\sigma_1=\lambda(e_1+e_3)+2\mu e_1\\\sigma_3=\lambda(e_1+e_3)+2\mu e_3\\\sigma_{13}=\mu e_{13}\end{aligned} \tag{14}$$

Here e_1, e_3, e_{13} the components of the deformation

$$e_1=\frac{\partial u_1}{\partial x_1},\ e_3=\frac{\partial u_3}{\partial x_3},\ e_{13}=\frac{\partial u_1}{\partial x_3}+\frac{\partial u_3}{\partial x_1} \tag{15}$$

The functions φ and ψ associated with movements are introduced in the usual way:

$$u_1=\frac{\partial\varphi}{\partial x_1}+\frac{\partial\psi}{\partial x_3},\quad u_1=\frac{\partial\varphi}{\partial x_3}-\frac{\partial\psi}{\partial x_1} \tag{16}$$

The equilibrium equations and formulas for stresses through functions φ and ψ can be written as follows:

$$\left(\nabla^2+h^2\right)\varphi=0\ ,\ \left(\nabla^2+k^2\right)\psi=0 \tag{17}$$

$$\begin{aligned}\sigma_1=\mu\left(-k^2\varphi-2\frac{\partial^2\varphi}{\partial x_3^2}+2\frac{\partial^2\psi}{\partial x_1\partial x_3}\right)\\\sigma_3=\mu\left(-k^2\varphi-2\frac{\partial^2\varphi}{\partial x_1^2}+2\frac{\partial^2\psi}{\partial x_1\partial x_3}\right)\\\sigma_{13}=\mu\left(-k^2\psi-2\frac{\partial^2\psi}{\partial x_1^2}+2\frac{\partial^2\psi}{\partial x_1\partial x_3}\right)\end{aligned} \tag{18}$$

$$\begin{aligned}h^2=\frac{\omega^2}{c_L^2},\quad k^2=\frac{\omega^2}{c_T^2},\\c_L=\sqrt{\frac{\lambda+2\mu}{\rho}},\quad c_T=\sqrt{\frac{\mu}{\rho}}\end{aligned} \tag{19}$$

Here, c_L and c_T are the phase velocities of longitudinal and transverse waves, h and k are the wave numbers of longitudinal and transverse waves, respectively.

To solve the problem, the integral Fourier transform of a variable x_1 is used

$$\begin{aligned}\varphi^*=\frac{1}{2\pi}\int_{-\infty}^{+\infty}\varphi e^{-i\xi x_1}dx_1\\\psi^*=\frac{1}{2\pi}\int_{-\infty}^{+\infty}\psi e^{-i\xi x_1}dx_1\end{aligned} \tag{20}$$

Since the axis x_3 is directed from the elastic half-space surface (Figure 1), the solution in the elastic half-space should decrease with x_3 decreasing, so the solution is taken as

$$\varphi^*=Ae^{\alpha x_3},\quad \psi^*=Be^{\beta x_3} \tag{21}$$

where α, β are positive real values, which ensures the attenuation of the stress-strain state of an elastic body when moving away from the source of vibrations deep into the body. The values α, β can be found as a result of

substituting (21) into equations (7), transformed taking into account the formulas (20)

$$\alpha = \sqrt{\xi^2 - h^2}\,, \qquad \beta = \sqrt{\xi^2 - k^2} \tag{22}$$

Equations (16), (19) as a result of applying the Fourier transform will take the form

$$\begin{aligned} u_1^* &= i\xi A e^{\alpha x_3} + \beta B e^{\beta x_3} \\ u_3^* &= \alpha A e^{\alpha x_3} - i\xi\beta e^{\beta x_3} \end{aligned} \tag{23}$$

$$\begin{aligned} \sigma_3^* &= \mu\left(\left(2\xi^2 - k^2\right) A e^{\alpha x_3} - 2i\xi\beta B e^{\beta x_3}\right) \\ \sigma_{13}^* &= \mu\left(\left(2\xi^2 - k^2\right) e^{\beta x_3} B - 2i\xi\alpha A e^{\alpha x_3}\right) \end{aligned} \tag{24}$$

Arbitrary integration constants A and B are found from the contact conditions of the sensor and the elastic half - space on the plane $x_3 = 0$.

The problem for an elastic half-space is solved using the integral Fourier transform. The integral stress σ_{31} conversion takes into account the equality of these stresses to the corresponding sensor stresses in the contact area and their equality to zero on the rest of the elastic body surface. A similar method is used in hydroacoustics to solve the problem of vibrations of a pivotally supported cylindrical shell immersed in an infinite liquid.

The first step of the iterative process is to solve the problem for a half-space when only a tangential load $\sigma_{31} = \sin px_1$ acts in the contact area on the surface of the half-space.

AUXILIARY PROBLEM FOR AN ELASTIC HALF-SPACE

The following stresses are set on the surface $x_3 = 0$ of an elastic body

$$\begin{aligned} &\sigma_{33}\big|_{x_3=0} = 0\,,\ \sigma_{13}\big|_{x_3=0} = X_{13}\,, \\ &X_{13} = \sin px_1\,,\ (|x_1| \le l)\,, \\ &\sigma_{33}\big|_{x_3=0} = 0\,,\ \sigma_{13}\big|_{x_3=0} = 0\,,\ (|x_1| > l)\,, \end{aligned} \tag{25}$$

With boundary conditions (25), N+1 auxiliary problems should be solved, in which $p=p_n=(2n+1)/2l$, n=0,1,2,...N. Then we write σ_{13} as a sum

$$\sigma_{13} = \sum_{n=0}^{N} C_n \sigma_{13} p_n x_1$$

with unknown constants c_n. The unknown constants c_n are determined by equating the sensor stress σ_{13} to the half-space stress σ_{13} in the contact area.

Using the Fourier transform (10), (11), (6), (9) reduces the conditions (25) to formulas

$$\sigma_3^*\big|_{x_3=0} = 0\,, \qquad \sigma_{13}^*\big|_{x_3=0} = X_{13}^*\,, \tag{26}$$

$$X_{13}^* = \frac{1}{4\pi}\left(\frac{e^{i(p+\xi)l} - e^{-i(p+\xi)l}}{p+\xi} - \frac{e^{i(p-\xi)l} - e^{-i(p-\xi)l}}{p-\xi}\right)$$

As a result of the Fourier transform, the conditions on the surface of the half- space $x_3 = 0$ will be written as

$$\begin{aligned} &(2\xi^2 - k^2)A - 2i\xi\beta B = 0, \\ &2i\xi\alpha A + (2\xi^2 - k^2)B = \frac{X_{13}^*}{\mu} \end{aligned} \tag{27}$$

where

$$A = \frac{2i\xi\beta}{F(\xi)}\frac{X_{13}^*}{\mu}\,, \quad B = \frac{2\xi^2 - k^2}{F(\xi)}\frac{X_{13}^*}{\mu} \tag{28}$$

To estimate the error of the sensor, the main interest is the displacement u_1 and the deformation e_1 on the surface of the half-space $x_3 = 0$, so we will write only the formula for u_1^*

$$u_1^* = \frac{\beta X_{13}^*}{\mu F(\xi)}(-2\xi^2 e^{\alpha x_3} + (2\xi^2 - k^2)e^{\beta x_3}) \tag{29}$$

$$u_1 = \frac{1}{\mu}\int_{-\infty}^{+\infty}(-2\xi^2 e^{\alpha x_3} + (2\xi^2 - k^2)e^{\beta x_3})\frac{\beta X_{13}^*}{F(\xi)} e^{i\xi x_1} d\xi \tag{30}$$

Integrals (29) in the contact area $|x_1| \le l$ can be transformed to a form convenient for calculations

$$u_1^{(n)} = -\frac{i}{2\mu} H_2^{(n)} e^{-i\kappa x_1} - \frac{i}{2\mu} P_2^{(n)} e^{-ipx_1} - \\ -\frac{i}{2\pi\mu} e^{-ikx_1} \int_0^\infty S_1 e^{-\eta x_1} d\eta - \frac{2i}{\pi\mu} e^{-ihx_1} \int_0^\infty S_2 e^{-\eta x_1} d\eta \quad (31)$$

here

$$H_2^{(n)} = -k^2 \beta_\kappa \frac{Z_1(-\kappa)}{F'(\kappa)}, \quad P_2^{(n)} = \frac{-k^2 \beta_P}{F(p)} \quad (32)$$

$$S_1^{(n)} = [4\varsigma^2 \Phi(\varsigma) - F(\varsigma) - F_1(\varsigma)] \frac{\beta \Phi(\varsigma)}{2F_2(\varsigma)} Z_1(\varsigma)\Big|_{\varsigma=-k+i\eta}$$

$$S_2^{(n)} = [F_1(\varsigma) - F(\varsigma) - 4\Phi(\varsigma)\alpha\beta] \frac{\varsigma^2 \beta}{4F_2(\varsigma)} Z_1(\varsigma)\Big|_{\varsigma=-h+i\eta}$$

$$Z_1(\varsigma) = \frac{e^{i(p+\varsigma)l}}{p+\varsigma} + \frac{e^{i(p-\varsigma)l}}{p-\varsigma}$$

NUMERICAL EXAMPLES OF CALCULATIONS FOR ESTIMATING THE ERROR OF THE STRAIN SENSOR

According to the general theory of deformation sensors, the elongation along the axis of the sensor is a constant value and is equal to the elongation on the surface of the half-space in the area of contact with the sensor. Then the movement of u_1 along the sensor changes linearly. The error of these assumptions is determined by calculating the displacement corrections u_1 found at the first step of the iterative process.

The sequence of calculations is as follows:

- calculate by formulas (31), (32) the displacement corrections u_1 as a function of the variable x_1 for problems with boundary conditions (25), where $p=p_n=(2n+1)/2l$, $n=0,1,2,...N$, - summarize the found corrections for n.

The results of the calculation are summarized in tables.

In all tables, the first column shows the values of the longitudinal displacements u_1 as a linear function of the variable x_1 obtained by the sensor as a result of the widely used assumption that the sensor does not change the SSS of the studied design. Columns 2-4 show the corrections for displacements obtained as a result of solving the contact problem. The sensor readings are correct if the corrections are significantly less than the displacement values in the first column. If the corrections are larger or of the same order as the movements written out in the first column, then this means that the sensor gives completely incorrect results.

Let us denote by $u_1^{(b)}$ the longitudinal displacement determined according to the accepted hypothesis that the sensor does not introduce disturbance into the stress-strain state of the structure under study. Let us denote by $u_1^{(c)}$ the corrections to $u_1^{(b)}$, obtained as a result of solving the contact problem.

Table 1. Values of displacements u_1 (first column) and corrections to them (columns 2-4) as functions of the variable x_1 and the circular frequency ω for a half-space made of steel and a sensor made of copper (sensor τ =0.002 m, l=0.02 m)

$u_1^{(b)}$	ω=1000	ω=10000	ω=100000
	$u_1^{(c)}$		
0.002	$5.5\cdot10^{-7}$	$6.2\cdot10^{-8}$	$10\cdot10^{-7}$
0.004	$1.3\cdot10^{-6}$	$3.3\cdot10^{-7}$	$1.6\cdot10^{-7}$
0.006	$2.2\cdot10^{-6}$	$1.1\cdot10^{-6}$	$2.9\cdot10^{-6}$
0.008	$3.1\cdot10^{-6}$	$2.0\cdot10^{-6}$	$6.6\cdot10^{-6}$
0.01	$4.1\cdot10^{-6}$	$3.0\cdot10^{-6}$	$1.1\cdot10^{-5}$
0.012	$5.0\cdot10^{-6}$	$4.1\cdot10^{-6}$	$1.6\cdot10^{-5}$
0.014	$5.8\cdot10^{-6}$	$5.1\cdot10^{-6}$	$2.0\cdot10^{-5}$
0.016	$6.5\cdot10^{-6}$	$6.1\cdot10^{-6}$	$2.5\cdot10^{-5}$
0.018	$7.2\cdot10^{-6}$	$7.0\cdot10^{-6}$	$2.9\cdot10^{-5}$
0.02	$7.7\cdot10^{-6}$	$7.8\cdot10^{-6}$	$3.4\cdot10^{-5}$

It can be seen from the table that the corrections are small, the error in the theory of strain sensors is less than 0.001%. It means that the

main hypothesis according to which the sensor introduces a small disturbance in the SSS of the studied structure is correct.

Table 2. Values of displacements u_1 (first column) and corrections to them (columns 2-4) as functions of the variable x_1 and the circular frequency ω for a half-space made of reinforced concrete and a sensor made of copper (sensor τ =0.002 m, l=0.02 m)

$u_1^{(b)}$	ω=50	ω=100	ω=500
	$u_1^{(c)}$		
0.002	0.0128	0.0075	-0.0253
0.004	0.0325	0.0240	-0.0244
0.006	0.0572	0.0470	-0.0041
0.008	0.0847	0.0740	0.0296
0.01	0.1129	0.1025	0.0715
0.012	0.1399	0.1304	0.1176
0.014	0.1646	0.1563	0.1653
0.016	0.1865	0.1797	0.2128
0.018	0.2058	0.2004	0.2593
0.02	0.2227	0.2190	0.3047

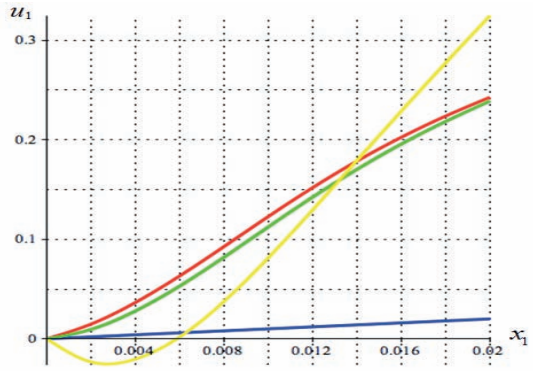

Figure 2. Displacement u_1 as a function of the variable x_1 in accordance with Table 2

The blue line on the Figure 2 corresponds to the displacement $u_1^{(b)}$ of Table 2 (column 1), the green line corresponds to the displacement $u_1^{(b)}$ taking into account the correction $u_1^{(c)}$ at ω=50 (Table 2, column 2), the red line - taking $u_1^{(b)}$ into account the correction $u_1^{(c)}$ at ω=100 (Table 2, column 3), the yellow line - $u_1^{(b)}$ taking into account the correction $u_1^{(c)}$ at ω=500 (Table 2, column 4).

The Figure 2 shows that in this case the sensor measurements are incorrect. The corrections $u_1^{(c)}$ are significantly greater than $u_1^{(b)}$.

Table 3. Values of displacements u_1 (first column) and corrections to them (columns 2-4) as functions of the variable x_1 and the circular frequency ω for a half-space made of reinforced concrete and a sensor made of constantan (sensor τ =0.0001 m, l=0.02 m)

$u_1^{(b)}$	ω=50	ω=100	ω=500
	$u_1^{(c)}$		
0.002	0.0010	0.0006	0.0019
0.004	0.0024	0.0018	0.0018
0.006	0.0043	0.0035	0.0003
0.008	0.0063	0.0055	0.0022
0.01	0.0084	0.0076	0.0053
0.012	0.0104	0.0097	0.0088
0.014	0.0123	0.0117	0.0123
0.016	0.0139	0.0134	0.0159
0.018	0.0154	0.0150	0.0194
0.02	0.0166	0.0163	0.0227

Tables 2, 3 show that the strain sensor introduces a large disturbance in the SSS of the studied structure, and gives incorrect values of deformations.

Table 4. Values of displacements u_1 (first column) and corrections to them (columns 2-4) as functions of the variable x_1 and the circular frequency ω for a half-space made of reinforced concrete and a sensor made of piezo film (sensor τ =0.0001 m, l=0.02 m)

$u_1^{(b)}$	ω=50	ω=100	ω=500
	$u_1^{(c)}$		
0.002	$2.9\cdot10^{-6}$	$1.7\cdot10^{-6}$	$-5.7\cdot10^{-6}$
0.004	$7.3\cdot10^{-6}$	$5.4\cdot10^{-6}$	$-5.5\cdot10^{-6}$
0.006	$1.3\cdot10^{-5}$	$1.1\cdot10^{-5}$	$9.2\cdot10^{-7}$
0.008	$1.9\cdot10^{-5}$	$1.7\cdot10^{-5}$	$6.6\cdot10^{-6}$
0.01	$2.5\cdot10^{-5}$	$2.3\cdot10^{-5}$	$1.6\cdot10^{-5}$

0.012	$3.1 \cdot 10^{-5}$	$2.9 \cdot 10^{-5}$	$2.6 \cdot 10^{-5}$
0.014	$3.7 \cdot 10^{-5}$	$3.5 \cdot 10^{-5}$	$3.7 \cdot 10^{-5}$
0.016	$4.2 \cdot 10^{-5}$	$4.0 \cdot 10^{-5}$	$4.8 \cdot 10^{-5}$
0.018	$4.6 \cdot 10^{-5}$	$4.5 \cdot 10^{-5}$	$5.8 \cdot 10^{-5}$
0.02	$5.0 \cdot 10^{-5}$	$4.9 \cdot 10^{-5}$	$6.8 \cdot 10^{-5}$

The results of the calculation in Table 4 show that the piezoelectric film deformation sensor causes a small disturbance in the SSS of the structure under study, and can be used to measure deformations in reinforced concrete structures.

CONCLUSION

The paper presents a relatively simple method for estimating the error of the theory of strain sensors.

It is shown by numerical examples that sensors made of materials with large elastic modules, used for structures made of materials with significantly smaller elastic modules, give incorrect measurements of deformations. This is confirmed by calculations performed for reinforced concrete structures. The calculation results allow us to recommend piezoelectric film sensors. Even more accurate measurements of deformations in reinforced concrete structures can be obtained using layered piezo film sensors [15]. Effective coefficients of this sensor must be obtained using the homogenization method [16]. Such a sensor has a smaller modulus of elasticity and a higher efficiency than a single-layer sensor.

Using the proposed method, it is possible to develop recomendations, which will specify the types of sensors for structures made of different materials that guarantee sufficiently correct measurements of deformations.

ACKNOWLEDGEMENTS

The research was funded by the National Research Moscow State University of Civil Engineering (grant for fundamental and applied scientific research, project No. 23-392/130).

REFERENCES

1. **Tomson W. (Lord Kelvin).** On the electrodynamic qualities of metals. Proc. R. Soc. London, 1856, no. 146, pp. 649–751.
2. **Infimovskaya A.A., Rogacheva N.N., Chernyshev G.N.** Use of thin piezoceramic gauges to measure dynamic deformations. Izv. Academy of Sciences of the USSR. MTT, 1989, Vol, 24, no. 2, pp.157-162.
3. **Rogacheva N., Sidorov V., Zheglova Yu.** Piezoelectric Sensor of Small Dynamic Bending Strains, Buildings 2024, Issue 14, Vol. 2447, doi:10.3390/buildings14082447.
4. **Li Y. Sharif-Khodaei Z.** Accuracy of Distributed Strain Sensing with Single-Mode Fibre in Composite Laminates under Thermal and Vibration Loads. Structural Control and Health Monitoring, 2023, no. 2, pp. 1-13, doi: 10.1155/2023/9269987.
5. **Calderon P., Glisic B.** Influence of mechanical and geometrical properties of embedded long-gauge strain sensors on the accuracy of strain measurement. IOP publishing Meas. Sci. Technol, 2012, Vol. 23, 065604, doi: 10.1088/0957-0233/23/6/065604.
6. **Zhao Y., Mengzhen L.** A theoretical strain transfer model analysis of the substrate-bonded FBG sensor considering the influence of groove. Journal of Instrumentation, Engineering, 2024, doi: 10.1088/1748-0221/19/09/p09005.
7. **Han D., Liu G., Xi Y., Zhao Y.** Theoretical analysis on the measurement accuracy of embedded strain sensor in asphalt pavement dynamic response monitoring based on FEM. Structural Control and Health Monitoring, 2022, Vol. 29, doi: 10.1002/stc.3140.
8. **Xinghao H. et al.** High-stretchability and low-hysteresis strain sensors using origami-inspired 3D mesostructures. Sci. Adv.,

2023, Vol. 9, 9799, doi: 10.1126/sciadv.adh9799.
9. **Aidong Q. et al.** Stretchable and calibratable graphene sensors for accurate strain measurement. Materials Advances, 2020, no. 1, pp. 235-243, doi: 10.1039/D0MA00032A.
10. **Shipunov G.S., Baranov M.A., Nikiforov A.S., Khabibrakhmanova F.R.** Comparison of mechanical strain measurement accuracy of fiberoptic sensor and smart-lay. Materials Physics and Mechanics, 2022, Vol. 48, no. 3, pp. 342-354, doi: 10.18149/MPM.4832022_5.
11. **Baldassarre A., Ocampo J., Martinez M., Rans C.** Accuracy of strain measurement systems on a non-isotropic material and its uncertainty on finite element analysis. Journal of Strain Analysis for Engineering Design, 2020, Vol. 56, Issue 2, pp. 76-95, doi: 10.1177/0309324720924580.
12. **Lamb H.**, Dynamic Theory of Sound, 2d edn, Edward Arnold (Publishers) Ltd., London, 1931, 307 p.
13. **Love A.E.H.**, Some Problems of Geodynamics, Cambridge University Press, Cambridge, UK, 1911.
14. **Kochetkov I.D., Rogacheva N.N.** Contact interaction of a piezoelectric actuator and elastic half-space. Journal of Applied Mathematics and Mechanics, 2005, Vol. 69, pp. 792-804.
15. **Rogacheva N.N.** Multilayered dynamic strain gauge using of piezoelectric PVDF films. MATEC Web of Conferences, 2017 Vol. 117, doi: 10.1051/matecconf/20 1711700146.
16. **Bensoussan A., Lions J.L., Papanicolaou G.** Asymptotic Analysis for Periodic Structures. American Mathematical Society, 2011, 392 p.

СПИСОК ЛИТЕРАТУРЫ

1. **Tomson W. (Lord Kelvin).** On the electrodynamic qualities of metals // Proc. R. Soc. London. 1856. № 146. pp. 649–751.
2. **Инфимовская А.А., Рогачева Н.Н., Чернышев Г.Н.** Использование тонких пьезокерамических датчиков для измерения динамических деформаций // Изв. Академия наук СССР. МТТ. 1989. Т. 24. вып. 2. с. 157-162.
3. **Rogacheva N., Sidorov V., Zheglova Yu.** Piezoelectric Sensor of Small Dynamic Bending Strains // Buildings. 2024. Issue 14. Vol. 2447, doi: 10.3390/buildings14082447.
4. **Li Y. Sharif-Khodaei Z.** Accuracy of Distributed Strain Sensing with Single-Mode Fibre in Composite Laminates under Thermal and Vibration Loads // Structural Control and Health Monitoring. 2023. № 2. pp. 1-13, doi: 10.1155/2023/9269987.
5. **Calderon P., Glisic B.** Influence of mechanical and geometrical properties of embedded long-gauge strain sensors on the accuracy of strain measurement // IOP publishing Meas. Sci. Technol. 2012. Vol. 23. 065604, doi: 10.1088/0957-0233/23/6/065604.
6. **Zhao Y., Mengzhen L.** A theoretical strain transfer model analysis of the substrate-bonded FBG sensor considering the influence of groove // Journal of Instrumentation, Engineering. 2024, doi: 10.1088/1748-0221/19/09/p09005.
7. **Han D., Liu G., Xi Y., Zhao Y.** Theoretical analysis on the measurement accuracy of embedded strain sensor in asphalt pavement dynamic response monitoring based on FEM // Structural Control and Health Monitoring. 2022. Vol. 29, doi: 10.1002/stc.3140.
8. **Xinghao H. et al.** High-stretchability and low-hysteresis strain sensors using origami-inspired 3D mesostructures // Sci. Adv. 2023. Vol. 9. 9799. doi: 10.1126/sciadv.adh9799.
9. **Aidong Q. et al.** Stretchable and calibratable graphene sensors for accurate strain measurement // Materials Advances.

2020. № 1. pp. 235-243, doi: 10.1039/D0MA00032A.
10. **Shipunov G.S., Baranov M.A., Nikiforov A.S., Khabibrakhmanova F.R.** Comparison of mechanical strain measurement accuracy of fiberoptic sensor and smart-lay // Materials Physics and Mechanics. 2022. Vol. 48. № 3. pp. 342-354, doi: 10.18149/MPM.4832022_5.
11. **Baldassarre A., Ocampo J., Martinez M., Rans C.** Accuracy of strain measurement systems on a non-isotropic material and its uncertainty on finite element analysis // Journal of Strain Analysis for Engineering Design. 2020. Vol. 56. Issue 2. pp. 76-95, doi: 10.1177/0309324720924580.
12. **Lamb H.**, Dynamic Theory of Sound, 2d edn, Edward Arnold (Publishers) Ltd. London. 1931. 307 p.
13. **Love A.E.H.**, Some Problems of Geodynamics, Cambridge University Press, Cambridge. UK. 1911.
14. **Kochetkov I.D., Rogacheva N.N.** Contact interaction of a piezoelectric actuator and elastic half-space // Journal of Applied Mathematics and Mechanics. 2005. Vol. 69. pp. 792-804.
15. **Rogacheva N.N.** Multilayered dynamic strain gauge using of piezoelectric PVDF films // MATEC Web of Conferences. 2017. Vol. 117, doi: 10.1051/matecconf/201711700146.
16. **Bensoussan A., Lions J.L., Papanicolaou G.** Asymptotic Analysis for Periodic Structures. American Mathematical Society. 2011. 392 p.

Rogacheva Nelly Nikolaevna — Doctor of Physical and Mathematical Sciences, Associate Professor of the Department of Computer Science and Applied Mathematics of the National Research Moscow State University of Civil Engineering; 129337, Russia, Moscow, Yaroslavskoe shosse, 26. E-mail: Rogachevann@mgsu.ru.

Рогачева Нэлля Николаевна — д.ф.-м.н., доцент кафедры Информатики и прикладной математики Национального исследовательского Московского государственного строительного университета; 129337, Россия, г. Москва, Ярославское шоссе, д. 26. E-mail: Rogachevann@mgsu.ru

Sidorov Vladimir Nikolaevich — Doctor of Technical Sciences, Professor, Academician of the Russian Academy of Sciences, Head of the Department of Computer Science and Applied Mathematics of the National Research Moscow State University of Civil Engineering; 129337, Russia, Moscow, Yaroslavskoe shosse, 26. E-mail: Sidorovvn@mgsu.ru

Сидоров Владимир Николаевич — д.т.н., профессор, академик РААСН, заведующий кафедрой Информатики и прикладной математики Национального исследовательского Московского государственного строительного университета; 129337, Россия, г. Москва, Ярославское шоссе, д. 26. E-mail: Sidorovvn@mgsu.ru

Zheglova Yulia Germanovna — Candidate of Technical Sciences, Associate Professor of the Department of Information Systems, Technologies and Automation in Construction of the National Research Moscow State University of Civil Engineering; 129337, Russia, Moscow, Yaroslavskoe shosse, 26. E-mail: Jeglovayug@mgsu.ru

Жеглова Юлия Германовна — к.т.н., доцент кафедры Информационных систем, технологий и автоматизации в строительстве Национального исследовательского Московского государственного строительного университета; 129337, Россия, г. Москва, Ярославское шоссе, д. 26. E-mail: Jeglovayug@mgsu.ru